Rare earth metals are essential for methanotrophic life in volcanic mudpots

Pol, A.; Barends, T.R.M.; Dietl, A.; Khadem, A.F.; Eygensteyn, J.; Jetten, M.S.M.; Camp, H.J.M. op den

2014, Article / Letter to editor (Environmental Microbiology, 16, 1, (2014), pp. 255-264)

Doi link to publisher: https://doi.org/10.1111/1462-2920.12249

environmental microbiology

Environmental Microbiology (2014) **16**(1), 255–264 doi:10.1111/1462-2920.12249

Rare earth metals are essential for methanotrophic life in volcanic mudpots

Arjan Pol,[1] Thomas R. M. Barends,[3] Andreas Dietl,[3] Ahmad F. Khadem,[1] Jelle Eygensteyn,[2] Mike S. M. Jetten[1]* and Huub J. M. Op den Camp[1]

Department of [1]Microbiology and [2]General Instruments, Radboud University Nijmegen, Heyendaalseweg 135, 6525 AJ, Nijmegen, The Netherlands.

[3]Department of Biomolecular Mechanisms, Max-Planck Institute for Medical Research, Jahnstrasse 29, D-69120 Heidelberg, Germany.

Summary

Growth of *Methylacidiphilum fumariolicum* SolV, an extremely acidophilic methanotrophic microbe isolated from an Italian volcanic mudpot, is shown to be strictly dependent on the presence of lanthanides, a group of rare earth elements (REEs) such as lanthanum (Ln), cerium (Ce), praseodymium (Pr) and neodymium (Nd). After fractionation of the bacterial cells and crystallization of the methanol dehydrogenase (MDH), it was shown that lanthanides were essential as cofactor in a homodimeric MDH comparable with one of the MDHs of *Methylobacterium extorquens* AM1. We hypothesize that the lanthanides provide superior catalytic properties to pyrroloquinoline quinone (PQQ)-dependent MDH, which is a key enzyme for both methanotrophs and methylotrophs. Thus far, all isolated MxaF-type MDHs contain calcium as a catalytic cofactor. The gene encoding the MDH of strain SolV was identified to be a *xoxF*-ortholog, phylogenetically closely related to *mxaF*. Analysis of the protein structure and alignment of amino acids showed potential REE-binding motifs in XoxF enzymes of many methylotrophs, suggesting that these may also be lanthanide-dependent MDHs. Our findings will have major environmental implications as metagenome studies showed (lanthanide-containing) XoxF-type MDH is much more prominent in nature than MxaF-type enzymes.

Received 10 June, 2013; revised 6 August, 2013; accepted 9 August, 2013. *For correspondence. E-mail m.jetten@science.ru.nl; Tel. (+31) (0) 24 365 2940; Fax (+31) (0) 24 365 2830.

Introduction

Members of the bacterial phylum Verrucomicrobia can be found in high numbers in a wide range of habitats including soils, insect guts, aquatic systems, marine sediments and hot springs (Wagner and Horn, 2006). Their physiology is largely unknown, and until recently, the (few) cultivated strains were described as anaerobic or aerobic heterotrophs. This changed with the discovery of methanotrophic Verrucomicrobia in geothermal regions (Dunfield *et al.*, 2007; Pol *et al.*, 2007; Islam *et al.*, 2008) for which the novel genus 'Methylacidiphilum' was proposed (Op den Camp *et al.*, 2009). They all are likely autotrophs (Khadem *et al.*, 2011; Sharp *et al.*, 2012) that use methane as an energy source and grow optimal between pH 2 and 5 at temperatures of 50–60°C. Besides representatives of the NC10 phylum, which have an intra-aerobic pathway (Ettwig *et al.*, 2010), the verrucomicrobial methanotrophs are the only known groups of aerobic methanotrophs outside of the Proteobacteria phylum. The representatives of the genus *Methylacidiphilum* are by far the most acidophilic (< pH 1) bacteria capable of methane oxidation.

When cultivating the verrucomicrobial methanotrophs, unknown factors seemed to limit growth under laboratory conditions in defined media, and this may have prevented their more frequent manifestation during enrichment and isolation studies of methanotrophs and methylotrophs from freshwater, marine and soil ecosystems (Chistoserdova *et al.*, 2009).

Rare earth elements (REEs) are essential for many high-tech devices like solar cells, mobile phones and computers. Although an exact role for them in biology is not known, some lanthanides, a group of REE such as lanthanum (Ln), cerium (Ce), praseodymium (Pr) and neodymium (Nd), were shown to affect various metabolic processes. Lanthanides are used as fertilizers in agriculture, and their positive effects have been attributed to interactions with ribulose-1,5-bisphosphate carboxylase/oxygenase (Liu *et al.*, 2011) and with the photosynthetic system, but the underlying mechanisms are poorly understood (Tyler, 2004). REEs are abundantly present in the earth's crust, but because of their low solubility, their concentration in most ecosystems does not exceed the nanomolar range. It has been suggested that the low

Table 1. REE in Solfatara mudpot water.

	Concentration (μM)	
Collection year	2011	2009
La	0.7	0.47
Ce	1.4	0.95
Pr	0.13	0.09
Nd	0.45	0.29
Sm	0.07	0.045
Eu	0.01	0.01
Gd	0.06	0.04
Total REE	2.8	1.9

biological availability of lanthanides has precluded the evolutionary development of lanthanide variants of metallo-enzymes, which were argued to be better alternatives to calcium (Franklin, 2001; Lim and Franklin, 2004). Recently, stimulation of *xox*F gene-encoded methanol dehydrogenase (MDH) expression in *Bradyrhizobium* sp. MAFF211645 and *Methylobacterium radiotolerans* by Ce(III) and La(III) has been reported (Fitriyanto *et al*., 2011; Hibi *et al*., 2011). Although the authors discussed the possibility of gene-level regulation by Ce, an Ln(III)-dependent MDH (XoxF-type) like the recently reported XoxF1 of *Methylobacterium extorquens* AM1 (Nakagawa *et al*., 2012) seems to be a more plausible explanation. This bacterium possesses also Ca(II)-dependent MDH (MxaF type), being the main enzyme catalysing methanol oxidation during growth on methanol. Lanthanides (III) have some similarities to calcium (II), such as ionic radius, coordination and ligand preferences. Especially for Ce, it is known that it can replace calcium in biomolecules or act as an antagonist, and as such is used in pharmacology (Jakupec *et al*., 2005).

In this study, we show the dependency on lanthanides for growth of *Methylacidiphilum fumariolicum* SolV. In addition, we purified, characterized and crystallized the Ln(III) containing MDH of this bacterium, and we discuss the environmental relevance of our findings.

Results and discussion

During our studies of *M. fumariolicum* SolV, we noticed that growth was very poor unless the medium was supplemented with mudpot water (MPW) from the Solfatara, its original habitat. No trace element with a known physiological role in biology could replace MPW. The final density obtained in the exponential growth phase was proportional to the amount of MPW added. Different batches of MPW resulted in varying responses, but addition of 1% v/v MPW (collected in 2011) resulted in exponential growth until an optical density of 0.5 at 600 nm (OD_{600}), after which growth continued in a linear mode. The growth-promoting compound in the MPW was evidently a mineral, as after evaporation of the water and ashing the residue (4 h at 550°C), it still promoted the growth of *M. fumariolicum* SolV. In search for the identity of this essential mineral, we analysed the trace metal composition of MPW, and of the supplemented medium before and after growth of *M. fumariolicum* SolV, by inductive coupled plasma mass spectrometry (ICP-MS). Thus, it could be established that REEs were present in MPW at concentrations of 2–3 μM (Table 1) much higher than in other ecosystems. Such high REE concentrations are typical for very acidic waters and are 100–1000 times higher compared with circumneutral surface or soil pore water and reflect their low solubility rather than their environmental abundance (Grawunder and Merten, 2012). The MPW and surrounding soils of the Solfatara have a very low pH (1–2) as a result of microbial production of sulphuric acid by oxidation of hydrogen sulfide present in the fumaroles. Hot sulfuric acid is actually used as extraction method in REE mining.

After exponential growth in medium containing 2% MPW, the REE had completely been removed by the *M. fumariolicum* SolV cells. Individually added REE salts (66 nM) could replace the MPW; SolV had consumed the supplemented La(III), Ce(III) or Pr(III) from the medium after the exponential growth had ceased. When the cells were grown with a range of Ce(III) concentrations, the stimulating activity was proportional to Ce(III) from 0 to 80 nM (Fig. 1). The OD_{600} obtained at the end of the exponential growth phase with 40 nM Ce(III) was 0.6, and this matched well with that obtained on MPW, considering the sum of La, Ce, Pr and Nd, the major REE present in

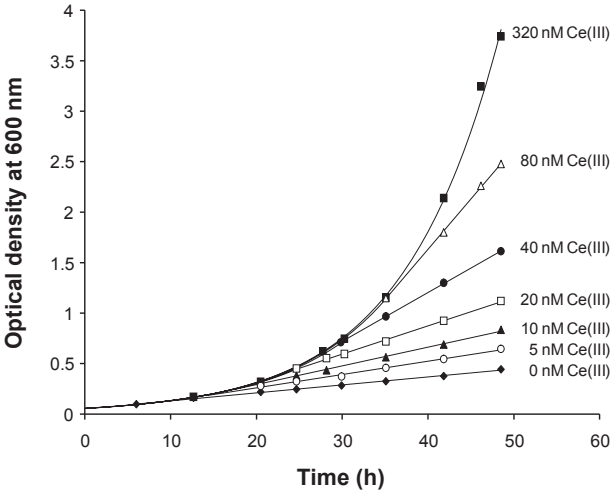

Fig. 1. Cerium-dependent growth of *Methylacidiphilum fumariolicum* SolV. At t = 0 bottles with different Ce(III) concentrations were inoculated with washed cells from a preculture until an optical density of 0.05. The preculture was grown on 100 nM of Ce(III). Data points are the average of two independent experiments.

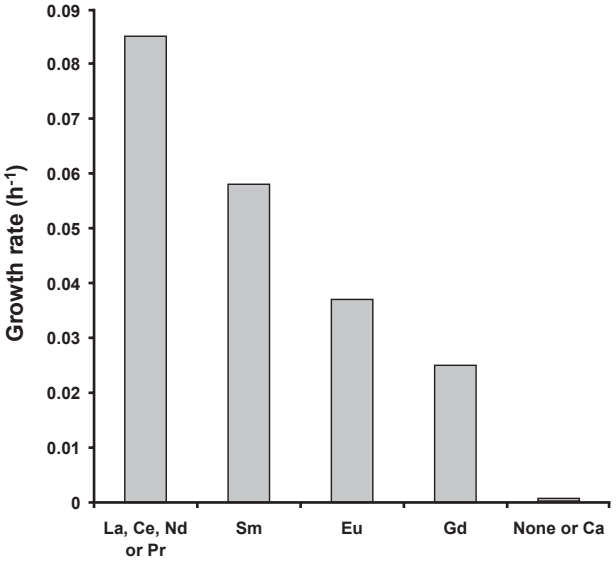

Fig. 2. Maximum growth rates with La, Ce, Pr, Nd and REE with higher atomic numbers tested individually at a concentration of 250 nM. Values are the mean of duplicate experiments, differing not more than 5%.

the MPW. When Ce(III) was added in excess, the uptake from the medium was 10-fold higher than needed for optimal growth. This may indicate that *M. fumariolicum* SolV may actively store this element. Another explanation would be adsorption to the cell wall. During growth in MPW-supplemented medium, Ce and La seem to disappear more quickly compared with Pr and Nd (Fig. S1). When tested individually, the maximum growth rates with these four REEs were identical. Salts of REE with higher atomic numbers than Nd were less supportive of growth. For example, with gadolinium, the doubling time of SolV had increased fourfold to 30 h (Fig. 2). The observation of a concentration dependent linear growth phase (Fig. 1) can only be explained assuming a limitation in the energy generating system with all structural biosynthesis routes unaffected.

In order to elucidate the exact role of the REE in *M. fumariolicum* SolV, we fractionated the proteins of SolV cells by cation exchange chromatography. Fractions containing MDH activity showed high REE concentrations. The pure MDH has an ultraviolet–visible (UV-Vis) spectrum (Fig. S2) with the features of dehydrogenases that contain cofactor PQQ (in its semiquinone oxidation state) (Anthony, 2000; 2004), but the peak typically present at around 345 nm had shifted to 354 nm. Calcium, the major metallic constituent of other MDHs, was below 10 mole % (Table 2) despite its presence (low mM range) both in the medium and MPW. Zn, Cu, Ba and Sr were also detected in the fractions. Of these, only Ba and Sr have been shown to be able to substitute Ca and produce active MDH (Goodwin and Anthony, 1996), but both metals did not stimulate growth of strain SolV. The highest signals in ICP-MS analysis were observed for the REEs La, Ce and Nd, which in total accounted for 0.6 atoms per MDH (monomer).

When *M. fumariolicum* SolV was cultivated in a medium without MPW but with only PrIII, a similarly active MDH with the same UV-Vis spectrum was purified from the resulting biomass. Metal analysis showed 0.5–0.7 Pr atoms per MDH monomer (Table 2). Again, Cu was found in relatively high amounts but seemed to be non-specifically bound because, in contrast to Pr, the copper content could be eightfold reduced upon washing the MDH with ethylenediaminetetraacetic acid (EDTA).

Sodium dodecylsulfate polyacrylamide gel electrophoresis (SDS-PAGE) of the purified MDH revealed a single band at 60 kDa (Fig. S2), and the gene encoding this protein was identified by matrix-assisted laser desorption/ionization time-of-flight mass spectrometry (MALDI-TOF MS) analysis of the band to be the *xox*F gene (Mfum_190005; 63 586 Da after SignalP (http://www.cbs.dtu.dk/services/SignalP/) predicted splicing) of the *xox*FGJ operon (Op den Camp *et al*., 2009). This operon is also present in the genome of *Methylacidiphilum infernorum* V4 (Hou *et al*., 2008). The *xox*F gene is the orthologue of *mxa*F that encodes the large subunit of typical MDHs. These MDH's are heterotetramers that contain a large and

Table 2. Metals in purified MDH of *Methylacidiphilum fumariolicum* SolV.

	Mole % of metals in MDH			
	MPW-MDH[a]		Pr-MDH[b]	
	Analysis 1	Analysis 2	No EDTA	EDTA
Ca[c]	< 10	< 5	< 8	< 8
Mn	5	4	n.a.	1
Cu	15	17	38	5
Zn	12	9	2	n.a.
Sr	1.8	1	< 1	< 1
Ba	8	9	2	2
La	19	21	–	–
Ce	26	27	–	–
Pr	n.a.	1.9	60–70	50–70
Nd	n.a.	4.5	–	–
Sm	n.a.	0.8	–	–
Eu	n.a.	0.1	–	–
Gd	n.a.	–	–	–

a. MDH purified from *M. fumariolicum* SolV after growth in medium supplemented with MPW; two samples were independently destructed with hot nitric acid and analysed by ICP-MS.
b. MDH purified from *M. fumariolicum* SolV after growth in medium supplemented with Pr(III). One sample with and one without EDTA treatment were destructed with hot nitric acid and analysed.
c. For Ca, the analysis was done by ICP-AES, which had lower background values than ICP-MS.
ICP-AES, inductively coupled plasma atomic emission spectroscopy; n.a., not analysed.<, below indicated value of the background; –, below detection level (0.1%).

Table 3. Kinetic parameters of purified MDH of *Methylacidiphilum fumariolicum* SolV.

Substrate	Affinity constant (μM)[a]	Maximum rate %[b]
Methanol	0.8 (± 0.3)	100
Ethanol	3	100
1-Propanol	7	100
1-Butanol	6	100
1-Hexanol	2	100
2-Propanol	–	0
Formaldehyde	7	100
Acetaldehyde	> 200	< 50
Formate	–	0

a. Affinity constant were obtained by best curve fitting of Michaelis–Menten kinetics as shown in Fig. S5. Values represent the average of a duplicate determination of which the individual values did not differ more then 20%. For methanol, the value is the average of five independent determinations of which the standard deviation is given in brackets.
b. Rate as compared with rate obtained for methanol as a substrate.

a small subunit ($\alpha_2\beta_2$). The small subunit is encoded by mxaI, which apparently is lacking from the *xox* operon of verrucomicrobial methanotrophs. In addition, the *xox*-operon of these methanotrophs lacks any accessory genes like *mxa*ACKLD shown to be involved in maturation/calcium insertion (Richardson and Anthony, 1992; Goodwin *et al.*, 1996; Toyama *et al.*, 1998). XoxFs are found in all available methylotroph genomes, but a clear role in methanol and/or formaldehyde oxidation has not been assigned as yet (Schmidt *et al.*, 2010; Chistoserdova, 2011).

The oligomeric state of purified MDH was assessed by analytical ultracentrifugation analysis which yielded an S-value of 7.1 which fitted best to a (dimeric) protein of 127 kD (Fig. S3). In the dye-linked assay, all MDHs reported so far showed hardly any activity without ammonium and required high pH (8–10) values (Anthony, 2000; 2004). In contrast, the MDH of *M. fumariolicum* SolV showed highest activity at neutral pH values (Fig. S4) and was completely independent of ammonium. Purified MDH displayed only very little endogenous substrate activity, and residual substrate was converted within a few minutes to produce virtual zero background rates. This made it possible to accurately measure the MDH kinetic properties for various substrates. The purified MDH had a temperature optimum around 60°C with a maximum specific activity of about 4 μmol·min^{-1} mg protein^{-1} which compares favourable with other MDHs. As reported for some other MDHs, primary alcohols and formaldehyde were oxidized at similar rates as methanol (Table 3). However, the affinity for methanol and the primary alcohols tested was much higher than those reported for other MDHs (affinity constants one order of magnitude lower). For methanol, an affinity constant as low as 0.8 μM was measured (Fig. S5), which is the lowest value reported ever for an MDH. When limiting amounts of methanol were added in the assay, almost twice the molar amounts (> 180%) of dye (dichlorophenolindophenol, DCPIP) were reduced, which indicates oxidation continues until to the level of formic acid. Other primary alcohols were oxidized to the respective aldehydes, reducing almost equimolar (> 90%) amounts of reduced DCPIP. Secondary alcohols and acetaldehyde were not oxidized. Our results, together with those reported by Nakagawa and colleagues (2012), clearly show that the XoxF-type enzymes are real MDH.

All of these highly unusual properties prompted us to determine the crystal structure of this MDH. The purified MDH was crystallized, and its structure was solved from a 1.6 Å resolution dataset (see Table S1) by molecular replacement using a model constructed from the *Methylobacterium extorquens* MDH structure (Ghosh *et al.*, 1995). The native enzyme appeared to be an asymmetric homodimer containing the PQQ cofactor (Fig. 3A). Calculations predict the sedimentation coefficient of the MDH dimer to be 7.0, which is very close to the experimental value (see above). Very high electron density consistent with a metal ion was present in each monomer of the MDH dimer. During refinement, it became apparent from both the density and the distances to the coordinating atoms (Table 4, Fig. 3B) that calcium, zinc, manganese and copper, found in MDH in low concentrations, could not account for the density in the metal binding sites. However, when Ce or Ln ions were placed in these positions instead, this resulted in good convergence when an occupancy of 0.6 was assumed for the lanthanide ions. No distance restraints were used at any time between the Ce or Ln ions and its coordinating atoms. Also, the planarity restraints on the PQQ O4 atoms had to be released to conform to the density, suggesting the PQQs to be in the radical semiquinone state (Anthony, 1996). Residual density in the active sites, coordinating the Ce/La-ions, was modelled as a (poly)-ethylene glycol fragment. A

Table 4. Distances to metal ion (Å).

Atom	Distance to Ce		Distance to Ca in MDH
	Ce A[a]	Ce B[a]	*M. extorquens*[b]
Glu^{172} OE1	2.7	2.6	2.4
Glu^{172} OE2	2.9	2.9	2.8
Asn^{256} OD1	2.7	2.7	3.1
Asp^{301} OD1	2.5	2.6	–
Asp^{301} OD2	2.8	2.7	–
Asp^{299} OD1	2.9	2.9	
PQQ O5	2.6	2.5	2.3
PQQ N6	2.8	2.8	2.3
PQQ O7	2.7	2.7	2.4
(poly)-ethylene glycol fragment O	2.8	3.0	

a. A and B refer to the two MDH monomers in the asymmetric unit.
b. Williams *et al.* (2005).

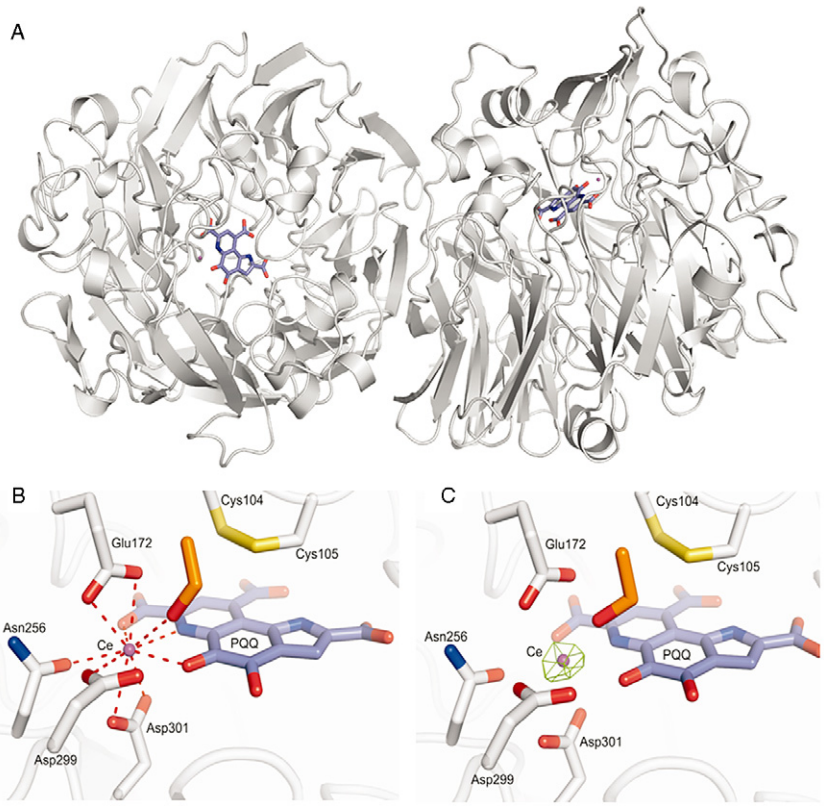

Fig. 3. X-ray crystal structure of *Methylacidiphilum fumariolicum* SolV methanol dehydrogenase.
A. Dimer structure with the PPQ shown in blue and the cerium ion in purple.
B. Close-up of the active site of MDH. The PQQ is shown in blue, the cerium ion in purple, the solvent molecule in orange and the coordination of the cerium ion is shown by red dashes.
C. Anomalous difference density (green mesh) calculated from data collected with 2.01074 Å wavelength radiation, contoured at 30 σ. A strong peak (35 σ) supports the presence of a cerium ion in the active site of MDH.

second dataset was collected at a wavelength of 2.01074 Å to search for the anomalous signal from any lanthanide ions present. An anomalous difference Fourier map calculated from these data indeed showed 35σ peaks at the positions of the ions (Fig. 3C), lending further support to the notion that these are lanthanide ions. In principle, barium ions could explain the electron density, the anomalous signal and the coordination distances; however, barium is present at 6- to 30-fold lower amounts (Table 2). We therefore conclude that the metal ions observed in the MDH crystal structure are lanthanide ions.

We speculate that the superior substrate affinity of lanthanide-containing MDH (Ln-MDH) is caused by the presence of lanthanides instead of Ca, as this was the most conspicuous change compared with Ca-MDH. All of the amino acids that coordinate PQQ and the metal ion were conserved, but the lanthanide is additionally coordinated by an asparagine (Asp^{301}), which replaces an alanine that is found in all MxaFs. Lanthanide ions are slightly bigger than calcium, and the extra space required seems to be created by some specific amino acid changes; proline (Pro^{259}), conserved in MxaF, is replaced by a threonine causing small changes in backbone conformations, which in turn force the upstream, coordinating Asn^{256} further away from the metal. A similar role is assumed for Gly^{171}, which replaces an alanine.

Although there is an ongoing debate on the exact mechanism of methanol oxidation by MDH, the catalytic centre is at carbon atoms C4 and C5 of the PQQ (Zhang *et al.*, 2007; Li *et al.*, 2011). Ca(II) is coordinated by protein carboxylate groups and three atoms of PQQ, one being the oxygen of the carbonyl at C5. It is commonly argued that Ca(II) acts as a Lewis acid and polarizes the carbonyl C5 atom of PQQ. Lanthanides (III) are much stronger Lewis acids than Ca(II) and thus are likely to render the C5 a stronger electrophile, making it easier to remove electrons from the substrate. This may explain the high rates of Ln-MDH observed at pH 7, reflecting the natural condition in the cell, without the need of ammonium activation at pH 9–11, and may be of great advantage for research on the mechanism of methanol oxidation. The high affinity and specific activity for formaldehyde of strain SolV Ln-MDH make a direct conversion of methanol to formate by Ln-MDH a likely route, without the need of additional methanopterin- or folate-dependent enzymes, which were shown to be absent or incomplete in the genome of strain SolV (Khadem *et al.*, 2012). In addition, we could not measure NAD(P)H or glutathione-depenedent formaldehyde conversion (results not shown).

As XoxF's are found much more frequently than MxaF-type MDHs and are present in all methylotrophs

(Chistoserdova, 2011), it is tempting to speculate that besides the MDHs from strain SolV (this study) and *Methylobacterium extorquens* AM1 (Nakagawa *et al*., 2012), more XoxF's are in fact lanthanide-containing high affinity MDH variants rather than low activity MDHs. This is further supported by the fact that the *xox*-operons lack accessory proteins required for maturation/calcium insertion (see above) and the conservation of the lanthanide-coordinating Asp^{301} in all XoxF branches. The occurrence of MxaF-type MDH in a phylogenetic tree as a subgroup in the XoxF-type enzymes (Chistoserdova, 2011) suggests that the latter type may be the primordial MDH.

A high affinity is crucial in environments where substrate concentrations are very low. In this respect, it is interesting to note that very high expression of the MDH-like XoxF proteins were encountered in the proteome of coastal oceanic microbial plankton (Sowell *et al*., 2011). Recently, methanol and other one carbon compound were demonstrated to be important substrates for bacterioplankton (OM43 clade) in coastal ecosystems (Giovannoni *et al*., 2008). The genome of the *Methylophilaceae* strain HTCC2181, a representative of this OM43 clade, was suggested to define a minimal gene set for methylotrophy and only possessed a XoxF type MDH (Giovannoni *et al*., 2008; Chistoserdova, 2011). Metagenome studies of Lake Washington sediment incubated with ^{13}C-methane suggested that the abundant *Methylophilaceae* phylotypes possessed multiple copies of *xox*F but lacked *mxa*FI genes (Kalyuzhnaya *et al*., 2008; Beck *et al*., 2013). These observations all point to an important role for the XoxF-type MDH in methanol oxidation under natural oligotrophic conditions.

The same very high expression of the MDH-like XoxF proteins was also reported for the phyllosphere of plants colonized by *Methylobacterium* spp. and *Methylobacterium extorquens* AM1 (Delmotte *et al*., 2009). Plants can bioconcentrate REE very efficiently (Weltje *et al*., 2002) and may provide the necessary amounts of lanthanides. In contrast, the low expression and activity of XoxF proteins in *Methylobacterium* under laboratory conditions are most likely caused by the lack of lanthanides in the medium used (Nakagawa *et al*., 2012). One might expect that the presence of Ln-MDH is not limited to methanotrophs or methylotrophs in acid geothermic locations and phyllospheres but will be more widely distributed in the environments where lanthanide concentrations are low but replenishable by sand, a practically infinite source of REE (Tyler, 2004 and references therein).

Experimental procedures

Strain, medium and culture conditions

Methylacidiphilum fumariolicum strain SolV was originally isolated from the central mudpot of the Solfatara crater (Pozzuoli, Italy) (Pol *et al*., 2007). The strain was grown on a mineral medium containing (in mM): NaH_2PO4, 1.0; $MgCl_2$, 0.2; $CaCl_2$, 0.2; Na_2SO_4, 1; K_2SO_4, 2; and $(NH_4)_2SO_4$, 2; trace elements (0.1% by volume) adjusted to pH 2.7 with sulfuric acid. MPW from the Solfatara crater (Pozzuoli, Italy) was centrifuged and filtered before use, and 1–4% was added to the medium. Incubation took place under a gas phase of air with 10% CH_4 and 5% CO_2 at 55°C and shaking at 400 r.p.m. Large-scale (10 l) cultivation was done as described by Khadem and colleagues (2012).

When testing REE dependency (salts > 99% pure), it was observed that standard serum bottles resulted in a highly variable growth, although exponential growth phase did never exceed OD_{600} 0.1 when no MPW or REE was added. Sand is one of the major raw materials of glass and may contain considerable amounts of REE, and Ce may be used as an additive during glass manufacturing. It was concluded that REEs in glass are extractable, at least partly, by the acidic media used. Better results were obtained with 250 ml polycarbonate Erlenmeyer flasks (Nalgene, Rochester, NY, USA), but it appeared that REE of previous usage remained attached to the inside of the these bottles as even after extensive machine washing and hot diluted acid rinsing variable background growth were observed. Best results were obtained with single use disposable polyethylene water bottles. In the screw caps, a hole was drilled in order to accommodate a red rubber septum needed for sampling. Contact of the acidic medium with needles used for sampling was minimized as the metal seems to release REE as well. For these experiments, concentrations of trace elements were (in μM): $NiCl_2$, 1; $CoCl_2$, 1; Na_2MoO_4, 1; $ZnSO_4$, 1; $FeSO_4$, 5; and $CuSO_4$, 10.

Purification of the MDH

Bacterial cells were harvested at late exponential phase by centrifugation, and the pellet was suspended in twice its volume of 10 mM phosphate buffer and adjusted to pH 7.2. DNA-ase I was added (30 mg l^{-1}), and cells were broken by two passages through a French press at 20 000 psi. Cell debris and membranes were removed by centrifugation at 30 000 × *g* for 1 h (Sorvall, GSA rotor at 4°C). The resulting clear supernatant, referred to as the cell-free extract, was used for purification of MDH and contained typically 30 mg ml^{-1} of protein. Up to 600 mg of cell-free extract protein was applied to an ice cooled SP-Sepharose-FF (GE Healthcare, Diegem, Belgium) cation exchange column (1.6 × 20 cm) (Liu *et al*., 2006) that was equilibrated in 10 mM sodium phosphate buffer, containing 1 mM methanol. The enzyme bound well to the column at pH values tested from pH 6 up to pH 7.5, despite a predicted pI value of 6.36. The column was washed at 2 ml min^{-1} with the equilibration buffer. Most of the proteins were not retained, and the absorbance (280 nm) went back to baseline after three column volumes have passed. Bound proteins were subsequently eluted with seven column volumes of a linear gradient of 0–500 mM NaCl in the same buffer. Best separation results were obtained at pH 7.2 at which MDH left the column at 190 mM NaCl as a symmetrical peak and with an activity yield of 85%. SDS-PAGE and MALDI-TOF MS analysis proved this peak to be virtually pure MDH. When methanol was not included

during this procedure, very little active MDH eluted from the column and a prominent turbid peak was eluted a bit later.

Specific activity of MDH increased 25-fold during purification. This factor is in accordance with the relatively large amount of MDH present in crude extract. The apparent MDH appeared as a dominant band in native PAGE of cell-free extract (Fig. S3), which after extraction and SDS-PAGE could be identified by MALDI-TOF MS analysis of a tryptic digest. Analysis of the native purified protein on MALDI-TOF MS revealed an average mass peak of 63 502 + 176 Da (SD, $n = 7$) corresponding with the calculated molecular mass (63 586 Da) of the protein encoded by gene Mfum_190005 after splicing of the signal peptide.

MDH activity assay

Initially, the assay was performed at high pH according to Anthony and Zatman (1967), but at lower pH values, the buffer was changed into 100 mM Tris-HCl or 20 mM sodium phosphate. Although at higher pH values the strain SolV MDH activity was stimulated by ammonium (40 mM), utmost twofold at pH 8, activity slowed down immediately from the start. At pH 9, MDH activity lasted just for a few seconds. Both phenazine methosulphate (PMS) and phenazine ethosulphate (PES) were used as primary electron acceptor. Both exhibited half saturation around 2–3 mM. Inhibition was observed at high concentration (> 5 mM). As PES gives much less background reduction of DCPIP, it was used in most cases, routinely at 1 mM. The assay was performed in a stirred 3 ml cuvette that contained 1.2 ml preheated reagents and was placed in a Cary spectrophotometer in a thermostatted holder. After adding the enzyme, DCPIP reduction was followed at 600 nm. When a stable rate was obtained, substrate was added and DCPIP reduction followed for maximally 1 min. The obtained rate was normalized to the maximum rate that was obtained with excess methanol added afterwards. In this way, we corrected for changes in enzyme activity during the day and for small variations like temperature between assays. For DCPIP, an extinction coefficient of 21.5 cm^{-1} mM^{-1} was taken at pH 8. The extinction (600 nm) change with pH was determined in order to correct for it. The estimated temperature optimum was around 60°C. Maximum specific activity was 4 μmol mg^{-1} min^{-1} when 2 mM PES was used, whereas at PES saturation, 8 μmol mg^{-1} min^{-1} was found. Higher temperatures were not tested because of the increasing background reactions. As reported for many other MDHs, reduction of DCPIP was observed without addition of a substrate (electron donor) like methanol, and this makes the determination of kinetic parameters cumbersome (Anthony, 2000). The source of this so-called endogenous substrate is still unclear. Buffers have been mentioned, and in our case, organic buffers like HEPES, TES, MES and PIPES apparently contained high amounts and prevented the measurement of methanol-dependent DCPIP reduction. With TRIS or phosphate buffer in the assay, endogenous reduction lasted for a few (2–4) minutes only. In contrast to other reports, cyanide did not inhibit this oxidation of endogenous substrate nor did it stimulate activity, but it stabilized MDH activity in the absence of methanol. The kinetics for substrates were studied at pH 7, and temperatures were between 40 and 45°C in order to limit chemical background reduction and reoxidation rates of DCPIP, especially with PMS. The choice for these parameters considerably increased the accuracy of slow rates at very low substrate concentrations. Noteworthy to mention that affinity constantly reported here were measured at 1 mM PES; however, occasionally, 2 mM was used, which seemed to result in about two times higher affinity constants. Initially, we measured the affinity constant for methanol with PMS in the assay and measured affinity constant values of around 0.5 μM; this is close to the detection limit of a spectrophotometer, and because of the higher background rates, accuracy was low. Again higher PMS concentration resulted in a higher affinity constant. Such an effect has been reported for PES with MDH of *Methylophilus methylotrophus* (Hothi *et al*., 2003), and the authors stated that subtraction of background 'endogenous' activity is inappropriate. However, the latter is done in many MDH kinetic studies and has significant influence on the outcome of kinetic parameters and makes direct comparison of reported values difficult.

Crystal structure

For crystallization, the protein was concentrated to an $A_{280}^{1\ cm}$ of 6.3 (corresponding to ~ 2.5 mg ml^{-1}) by ultrafiltration in 25 mM HEPES/NaOH, pH 7.5, 25 mM KCl, 1 mM methanol. Initial crystals were obtained in 100 + 100 nl sitting drops using a reservoir solution containing 20%w/v polyethylene glycol (PEG) 8000, 0.2 M NaCl, 0.1 M N-cyclohexyl-3-aminopropanesulfonic acid (CAPS) (NaOH) pH 10.5. This condition was optimized in 1 + 1 μl hanging drops using 600 μl of 22%w/v PEG 8000, 0.2 M NaCl, without buffer, in Linbro plates. Crystals were cryoprotected by briefly soaking them in reservoir solution with 30% (v/v) ethylene glycol and then flash-cooled in liquid nitrogen. All crystallographic data were measured at the X10SA beamline (at a wavelength of 0.9718 Å and 2.01074 Å) of the Swiss Light Source at the Paul-Scherrer Institut in Villigen, Switzerland, and data were processed with XDS (Kabsch, 1988a,b; 1993; 2010a,b). The structure was solved from the 1.6 Å resolution dataset (see Table 1) by molecular replacement with PHASER (McCoy *et al*., 2005) using a model constructed by MolRep (Vagin and Teplyakov, 1997) from the *Methylobacterium extorquens* MDH structure Ghosh *et al*., 1995). Refinement was performed using Refmac (Murshudov *et al*., 1997) and PHENIX (Adams *et al*., 2010) with iterative rebuilding done in COOT (Emsley and Cowtan, 2004).

Riding hydrogen atoms and anisotropic B-factors for the Ce ions were used to obtain the final model. Despite the use of anisotropic B-factor refinement for the Ce ions, some residual difference density remains around the Ce ions, likely because of either the partial occupancy or the fact that the metal binding sites likely contain a mixture of lanthanides, or both.

The final, refined model shows excellent geometry, although 0.3% of residues have unfavourable Ramachandran angles as determined by MolProbity (Chen *et al*., 2010). However, inspection of the electron density for these residues showed no discrepancies between density and model. Structural figures were prepared using PyMol (http://www.pymol.org).

Analytical ultracentrifugation

MDH was concentrated to $A_{280}^{1\ cm} = 6.3$ in 25 mM HEPES/NaOH, pH 7.5, 25 mM KCl, 1 mM methanol and investigated in a Beckman Proteomelab XL-I (Beckmann Coulter GmbH, Krefeld, Germany) analytical ultracentrifuge at 30 000 r.p.m. and 20°C in a two-sector cell with a 1.2 cm optical path length. Absorption scan data were collected at 280 nm and evaluated using SEDFIT (Schuck, 2009). Assuming a monomer with a molecular weight (MW) of 63 586 Da as calculated from the sequence, maximum possible sedimentation coefficients $S_{max} \approx 0.00361.MW^{2/3}$ of 12.0, 9.1 and 5.8 can be estimated for an MDH trimer, dimer and monomer respectively (Erickson, 2009). As the main maximum in the c(S) distribution of MDH was at 7.1 Svedberg, these values correspond to S_{max}/S values of 1.7, 1.3 and 0.8, respectively, indicating that MDH most probably occurs as a dimer in solution (Erickson, 2009). Indeed, calculations with HYDROPRO, García de la Torre and colleagues (2000) predict the sedimentation coefficient of the MDH dimer found in the crystal structure to be 7.0, which is very close to the experimental value.

Metal analysis by ICP-MS and ICP-optical emission spectrometry (OES)

Metals were analysed by ICP-MS on a Series I ICP MS (Thermo Scientific, Breda, the Netherlands). Ca measurements were done by ICP_OES on a iCap 6300 radial (Thermo Scientific). Height point calibration was performed with a dilution series of (multi-) element standards (1000 ppm in 1% nitric acid; Merck, Darmstadt, Germany). For metals present in MDH, 50–300 µl of purified MDH (9.7 mg protein ml^{-1} for MPW-MDH or 7.0 mg protein ml^{-1} for Pr-MDH) was washed with water on a Vivaspin 500 filter (Sartorius, Goettingen, Germany) and destructed with nitric acid (10–30%) at 90°C for 30–60 min and diluted to 5 ml with water.

Protein determination

Protein in cell-free extract was determined by the bicinchonic acid (BCA) Protein Assay kit (Pierce, Rockford, IL, USA), with serum albumin as a standard. The protein concentration of purified MDH was determined by its extinction at 280 nm. The molar extinction coefficient 158 cm^{-1} mM^{-1} was calculated on basis of its deduced amino acid sequence with the 'Protein Identification and Analysis Tools' on the ExPASy Server (http://www.expasy.ch/tools). MDH protein concentration measured by the Biorad assay was 50% higher or lower (with gamma globulin and BSA as standards respectively)

MALDI-TOF MS analysis

The molecular mass and identification of MDH in SDS-PAGE gels were determined MALDI-TOF MS on gel spots as described previously (Khadem *et al*., 2011).

Acknowledgements

The work was funded by a Mosaic grant (017.005.113) of the Netherlands Organization for Scientific Research to A.F. Khadem, by an European Research Council grant (232937) to M.S.M. Jetten and by the Max-Planck Society. T.R.M. Barends wishes to thank Ilme Schlichting for continuous support and collection of diffraction data.

Author information

Atomic coordinates and structure factor amplitudes have been deposited in the PDB with accession code 4MAE.

References

Adams, P.D., Afonine, P.V., Bunkóczi, G., Chen, V.B., Davis, I.W., Echols, N., *et al*. (2010) PHENIX: a comprehensive Python-based system for macromolecular structure solution. *Acta Crystallogr D Biol Crystallogr* **66:** 213–221.

Anthony, C. (1996) Quinoprotein-catalysed reactions. *Biochem J* **320:** 697–711.

Anthony, C. (2000) Methanol dehydrogenase, a PQQ-containing quinoprotein dehydrogenase. *Subcell Biochem* **35:** 73–117.

Anthony, C. (2004) The quinoprotein dehydrogenases for methanol and glucose. *Arch Biochem Biophys* **428:** 2–9.

Anthony, C., and Zatman, L.J. (1967) The microbial oxidation of methanol. Purification and properties of the alcohol dehydrogenase of *Pseudomonas* sp. M27. *Biochem J* **104:** 953–959.

Beck, D.A.C., Kalyuzhnaya, M.G., Malfatti, S., Tringe, S.G., Glavina del Rio, T., Ivanova, N., *et al*. (2013) A metagenomic insight into freshwater methane-utilizing communities and evidence for cooperation between the *Methylococcaceae* and the *Methylophilaceae*. *Peerj* **1:** e23.

Chen, V.B., Arendall, W.B., Headd, J.J., Keedy, D.A., Immormino, R.M., Kapral, G.J., *et al*. (2010) MolProbity: all-atom structure validation for macromolecular crystallography. *Acta Crystallogr D Biol Crystallogr* **66:** 12–21.

Chistoserdova, L. (2011) Modularity of methylotrophy, revisited. *Environ Microbiol* **13:** 2603–2622.

Chistoserdova, L., Kalyuzhnaya, M.G., and Lidstrom, M.E. (2009) The expanding world of methylotrophic metabolism. *Annu Rev Microbiol* **63:** 477–499.

Delmotte, N., Knief, C., Chaffron, S., Innerebner, G., Roschitzki, B., Schlapbach, R., *et al*. (2009) Community proteogenomics reveals insights into the physiology of phyllosphere bacteria. *Proc Natl Acad Sci USA* **106:** 16428–16433.

Dunfield, P.F., Yuryev, A., Senin, P., Smirnova, A.V., Stott, M.B., Hou, S., *et al*. (2007) Methane oxidation by an extremely acidophilic bacterium of the phylum Verrucomicrobia. *Nature* **450:** 879–882.

Emsley, P., and Cowtan, K. (2004) Coot: model-building tools for molecular graphics. *Acta Crystallogr D Biol Crystallogr* **60:** 2126–2132.

Erickson, H.P. (2009) Size and shape of protein molecules at the nanometer level determined by sedimentation, gel filtration, and electron microscopy. *Biol Proced Online* **11:** 32–51.

Ettwig, K.F., Butler, M.K., Le Paslier, D., Pelletier, E., Mangenot, S., Kuypers, M.M.M., *et al*. (2010) Nitrite-driven

anaerobic methane oxidation by oxygenic bacteria. *Nature* **464:** 543–548.

Fitriyanto, N.A., Fushimi, M., Matsunaga, M., Pertiwiningrum, A., Iwama, T., and Kawai, K. (2011) Molecular structure and gene analysis of Ce^{3+}-induced methanol dehydrogenase of *Bradyrhizobium* sp. MAFF211645. *J Biosci Bioeng* **111:** 613–617.

Franklin, S.J. (2001) Lanthanide-mediated DNA hydrolysis. *Curr Opinion Chem Biol* **5:** 201–208.

García de la Torre, J., Huertas, M.L., and Carrasco, B. (2000) Calculation of hydrodynamic properties of globular proteins from their atomic-level structure. *Biophys J* **78:** 719–730.

Ghosh, M., Anthony, C., Harlos, K., Goodwin, M.G., and Blake, C. (1995) The refined structure of the quinoprotein methanol dehydrogenase from *Methylobacterium extorquens* at 1.94 Å. *Structure* **3:** 177–187.

Giovannoni, S.J., Hayakawa, D.H., Tripp, H.J., Stingl, U., Givan, S.A., Cho, J.C., *et al*. (2008) The small genome of an abundant coastal ocean methylotroph. *Environ Microbiol* **10:** 1771–1782.

Goodwin, M.G., and Anthony, C. (1996) Characterization of a novel methanol dehydrogenase containing a Ba^{2+} ion at the active site. *Biochem J* **318:** 673–679.

Goodwin, M.G., Avezoux, A., Dales, S.L., and Anthony, C. (1996) Reconstitution of the quinoprotein methanol dehydrogenase from inactive Ca^{2+}-free enzyme with Ca^{2+}, Sr^{2+} or Ba^{2+}. *Biochem J* **319:** 839–842.

Grawunder, A., and Merten, D. (2012) Rare earth elements in acidic systems – niotic and abiotic impacts. *Soil Biol* **31:** 81–97.

Hibi, Y., Asai, K., Arafuka, H., Hamajima, M., Iwama, T., and Kawai, K. (2011) Molecular structure of La^{3+}-induced methanol dehydrogenase-like protein in *Methylobacterium radiotolerans*. *J Biosci Bioeng* **111:** 547–549.

Hothi, P., Basran, J., Sutcliffe, M.J., and Scrutton, N.S. (2003) Effects of multiple ligand binding on kinetic isotope effects in PQQ-dependent methanol dehydrogenase. *Biochemistry* **42:** 3966–3978.

Hou, S., Makarova, K.S., Saw, J.H., Senin, P., Ly, B.V., Zhou, Z., *et al*. (2008) Complete genome sequence of the extremely acidophilic methanotroph isolate V4, *Methylacidiphilum infernorum*, a representative of the bacterial phylum Verrucomicrobia. *Biol Direct* **3:** 26.

Islam, T., Jensen, S., Reigstad, L.J., Larsen, O., and Birkeland, N.K. (2008) Methane oxidation at 55 degrees C and pH 2 by a thermoacidophilic bacterium belonging to the Verrucomicrobia phylum. *Proc Natl Acad Sci USA* **105:** 300–304.

Jakupec, M.A., Unfried, P., and Keppler, B.K. (2005) Pharmacological properties of cerium compounds. *Rev Physiol Biochem Pharmacol* **153:** 101–111.

Kabsch, W. (1988a) Evaluation of single crystal X-ray diffraction data from a position sensitive detector. *J Appl Crystallogr* **21:** 916–924.

Kabsch, W. (1988b) Automatic indexing of rotation diffraction patterns. *J Appl Crystallogr* **21:** 67–71.

Kabsch, W. (1993) Automatic processing of rotation diffraction data from crystals of initially unknown symmetry and cell constants. *J Appl Crystallogr* **26:** 795–800.

Kabsch, W. (2010a) XDS. *Acta Crystallogr Section D Biol Crystallogr* **66:** 125–132.

Kabsch, W. (2010b) Integration, scaling, space-group assignment and post-refinement. *Acta Crystallogr Section D Biol Crystallogr* **66:** 133–144.

Kalyuzhnaya, M.G., Lapidus, A., Ivanova, N., Copeland, A.C., McHardy, A.C., Szeto, E., *et al*. (2008) High resolution metagenomics targets major functional types in complex microbial communities. *Nature Biotech* **26:** 1029–1034.

Khadem, A.F., Pol, A., Wieczorek, A., Mohammadi, S.S., Francoijs, K.J., Stunnenberg, H.G., *et al*. (2011) Autotrophic methanotrophy in verrucomicrobia: *Methylacidiphilum fumariolicum* SolV uses the Calvin-Benson-Bassham cycle for carbon dioxide fixation. *J Bacteriol* **193:** 4438–4446.

Khadem, A.F., van Teeseling, M.C., van Niftrik, L., Jetten, M.S.M., Op den Camp, H.J.M., and Pol, A. (2012) Genomic and physiological analysis of carbon storage in the verrucomicrobial methanotroph 'Ca. *Methylacidiphilum fumariolicum*' SolV. *Front Microbiol* **3:** 345.

Li, J., Gan, J.H., Mathews, F.S., and Xia, Z.X. (2011) The enzymatic reaction-induced configuration change of the prosthetic group PQQ of methanol dehydrogenase. *Biochem Biophys Res Commun* **406:** 621–626.

Lim, S., and Franklin, S.J. (2004) Lanthanide-binding peptides and the enzymes that Might Have Been. *Cell Mol Life Sci* **61:** 2184–2188.

Liu, C., Hong, F.S., Tao, Y., Liu, T., Xie, Y.N., Xu, J.H., and Li, Z.R. (2011) The mechanism of the molecular interaction between cerium (III) and ribulose-1,5-bisphosphate carboxylase/oxygenase (Rubisco). *Biol Trace Elem Res* **143:** 1110–1120.

Liu, Q., Kirchhoff, J.R., Faehnle, C.R., Viola, R.E., and Hudson, R.A. (2006) A rapid method for the purification of methanol dehydrogenase from *Methylobacterium extorquens*. *Protein Expr Purif* **46:** 316–320.

McCoy, A., Grosse-Kunstleve, R.W., Storoni, L.C., and Read, R.J. (2005) Likelihood-enhanced fast translation functions. *Acta Crystallogr Section D Biol Crystallogr* **61:** 458–464.

Murshudov, G.N., Vagin, A.A., and Dodson, E.J. (1997) Refinement of macromolecular structures by the maximum-likelihood method. *Acta Crystallogr Section D Biol Crystallogr* **53:** 240–255.

Nakagawa, T., Mitsui, R., Tani, A., Sasa, K., Tashiro, S., Iwama, T., *et al*. (2012) A catalytic role of XoxF1 as La^{3+}-dependent methanol dehydrogenase in *Methylobacterium extorquens* strain AM1. *PLoS ONE* **7:** e50480.

Op den Camp, H.J.M., Islam, T., Stott, M., Harhangi, H.R., Hynes, A., Schouten, S., *et al*. (2009) Environmental, genomic and taxonomic perspectives on methanotrophic *Verrucomicrobia*. *Environ Microbiol Rep* **1:** 293–306.

Pol, A., Heijmans, K., Harhangi, H.R., Tedesco, D., Jetten, M.S.M., and Op den Camp, H.J.M. (2007) Methanotrophy below pH 1 by a new Verrucomicrobia species. *Nature* **450:** 874–878.

Richardson, I.W., and Anthony, C. (1992) Characterization of mutant forms of the quinoprotein methanol dehydrogenase lacking an essential calcium ion. *Biochem J* **287:** 709–715.

Schmidt, S., Christen, P., Kiefer, P., and Vorholt, J.A. (2010) Functional investigation of methanol dehydrogenase-like protein XoxF in *Methylobacterium extorquens* AM1. *Microbiology* **156:** 2575–2586.

Schuck, P. (2009) Size distribution analysis of macromolecules by sedimentation velocity ultracentrifugation and Lamm equation modeling. *Biophys J* **78:** 1606–1619.

Sharp, C.E., Stott, M.B., and Dunfield, P.F. (2012) Detection of autotrophic verrucomicrobial methanotrophs in a geothermal environment using stable isotope probing. *Front Microbiol* **3:** 303.

Sowell, S.M., Abraham, P.E., Shah, M., Verberkmoes, N.C., Smith, D.P., Barofsky, D.F., and Giovannoni, S.J. (2011) Environmental proteomics of microbial plankton in a highly productive coastal upwelling system. *ISME J* **5:** 856–865.

Toyama, H., Anthony, C., and Lidstrom, M.E. (1998) Construction of insertion and deletion *mxa* mutants of *Methylobacterium extorquens* AM1 by electroporation. *FEMS Microbiol Lett* **166:** 1–7.

Tyler, G. (2004) Rare earth elements in soil and plant systems – a review. *Plant Soil* **267:** 191–206.

Vagin, A., and Teplyakov, A. (1997) MOLREP: an automated program for molecular replacement. *J Appl Crystallogr* **30:** 1022–1025.

Wagner, M., and Horn, M. (2006) The Planctomycetes, Verrucomicrobia, Chlamydiae and sister phyla comprise a superphylum with biotechnological and medical relevance. *Curr Opin Biotechnol* **17:** 241–249.

Weltje, L., Heidenreich, H., Zhu, W., Wolterbeek, H.T., Korhammer, S., de Goeij, J.J.M., and Markert, B. (2002) Lanthanide concentrations in freshwater plants and molluscs, related to those in surface water, pore water and sediment. A case study in The Netherlands. *Sci Total Environ* **286:** 191–214.

Williams, P.A., Coates, L., Mohammed, F., Gill, R., Erskine, P.T., Coker, A., *et al*. (2005) The atomic resolution structure of methanol dehydrogenase from *Methylobacterium extorquens*. *Acta Crystallogr D Biol Crystallogr* **61:** 75–79.

Zhang, X., Reddy, S.Y., and Bruice, T.C. (2007) Mechanism of methanol oxidation by quinoprotein methanol dehydrogenase. *Proc Natl Acad Sci USA* **104:** 745–749.

Supporting information

Additional Supporting Information may be found in the online version of this article at the publisher's web-site:

Fig. S1. Uptake preference within the series of REE (La, Ce, Pr, Nd) during growth in MPW-supplemented (4%) medium.
Fig. S2. SDS-PAGE (12%) of the purified methanol dehydrogenase of strain SolV (A) and the UV-Vis spectrum of the pure enzyme (B).
Fig. S3. Analytical ultracentrifugation analysis of purified MDH.
Fig. S4. Effect of pH on MDH activity. Activities refer to the μM DCPIP reduced per min. Each symbol represents an individual measurement. Squares and triangles indicate measurements with and without 40 mM ammonium chloride respectively.
Fig. S5. A. Kinetics of purified MDH. Symbols indicate individual rate measurements. Lines represent the curves obtained by fitting Michaelis–Menten kinetics. Obtained affinity constants (Km) are given in Table 3.
B. Kinetics of purified MDH. Symbols indicate individual rate measurements. Lines represent the curves obtained by fitting Michaelis–Menten kinetics. Obtained affinity constants (Km) are given in Table 3.
Table S1. Crystallographic data and model quality.